



Concentration Dependence of VO²⁺ Crossover of Nafion for Vanadium Redox Flow Batteries

Jamie S. Lawton,^a Amanda Jones,^a and Thomas Zawodzinski^{a,b,*}

^aDepartment of Chemical and Biomolecular Engineering, University of Tennessee at Knoxville, Knoxville, Tennessee 37996, USA

^bMaterials Science and Technology Division, Oak Ridge National Laboratory, Oak Ridge, Tennessee 37831, USA

The VO²⁺ crossover, or permeability, through Nafion in a vanadium redox flow battery (VRFB) was monitored as a function of sulfuric acid concentration and VO²⁺ concentration. A vanadium rich solution was flowed on one side of the membrane through a flow field while symmetrically on the other side a blank or vanadium deficit solution was flowed. The blank solution was flowed through an electron paramagnetic resonance (EPR) cavity and the VO²⁺ concentration was determined from the intensity of the EPR signal. Concentration values were fit using a solution of Fick's law that allows for the effect of concentration change on the vanadium rich side. The fits resulted in permeability values of VO²⁺ ions across the membrane. Viscosity measurements of many VO²⁺ and H₂SO₄ solutions were made at 30–60°C. These viscosity values were then used to determine the effect of the viscosity of the flowing solution on the permeability of the ion.

© 2013 The Electrochemical Society. [DOI: 10.1149/2.004306jes] All rights reserved.

Manuscript submitted December 5, 2012; revised manuscript received January 29, 2013. Published February 22, 2013.

The Vanadium Redox Flow Battery (VRFB) is an energy storage device consisting of flowing anolyte (V(II)/V(III)) and catholyte (VO²⁺/VO²⁺) often separated by an ion exchange membrane, such as Nafion.¹ Across the literature on VRFBs there are many variations in vanadium concentrations and H₂SO₄ concentrations used in battery operation.^{2–4} Vanadium diffusion through the membrane, or crossover, is a problem that leads to electrolyte imbalances and self discharge of the battery.⁵ Many alternative membranes have been studied for applications in VRFBs with a primary goals to minimize crossover and cost.⁶ In addition to cross-over, internal cell resistance in high-performance cells is often dominated by the membrane resistance. Water and acid transport during cell operation also can be significant, leading to operational problems. Thus, probing and understanding mass transport effects in or through membranes is of great importance to the advancement of the technology.

The uptake of water, acid and ions is the critical background on which any consideration of mass transport effects must be based. Verbrugge and co-workers^{7,8} published experimental studies and models of sulfuric acid and water uptake and transport in Nafion and observed a drop in the diffusion coefficient of the bisulfate ion at a H₂SO₄ concentration of 3 M. A recent study characterizing the effects of vanadium⁹ on Nafion have observed slower motional rates with higher vanadium contents in the membrane. Experiments detailing the effects of sulfuric acid interaction with the membrane have reported membrane dehydration at increasing sulfuric acid concentrations.⁷

One important use of uptake and mass transport data is as input for modeling of key phenomena occurring in the VRFB cells. Recent modeling efforts have varied in their approach to the membrane and in their access to transport data.^{10–13} The data available as input is often derived based on a partial or scattershot group of measurements. Typically, these data are not obtained from experiments taking into account the nature of the transport problem in concentrated solutions. Values used do not always reflect the environment in the operating cell or are based on measurements intended for fuel cell operations, which do not necessarily compare to VRFB conditions. Some models have focused on modeling the overall cell while downplaying the membrane-related aspects of operation. While such models, usually based on CFD calculations allow some consideration of the physical aspects of the cell (mass transport in channels and in porous media), they are mostly simplistic in their consideration of membrane effects. Unfortunately, this limits the insight gained since several of the most important aspects of cell performance are dominated by membrane transport phenomena.

The transport phenomena in the membranes used in VRFBs is extremely complex on the face of it. First, there are a large num-

ber of components, all (more or less) present in the 'concentrated solution' regime. This regime requires explicitly including variable activity coefficient effects or inter-component interactions. With 4 vanadium species, protons, bisulfate and water to consider, one would need at least 21 independent parameters to fully describe the transport processes. Looked at in another way, the transport of each species interacts with that of the others. In this light, measurements using a simple Fickian description of transport of a single component, the dilute solution transport limit, provides diffusion data of limited utility unless carried out over a wide range of systematically varied conditions.

This contribution is the first in a projected series of papers that will provide data and analysis to support modeling and concentrated solution theory analysis of VRFB cell and membrane processes. Here, we report a primary set of data for diffusion of vanadium across Nafion membranes using Electron Paramagnetic Resonance (EPR) as a detector of species concentrations. We have simplified the transport problem for this work to include only a single vanadium species (VO²⁺) in the presence of sulfuric acid. Even with just the single ion being considered, there are substantial complications in the description of the transport process. We have carried out measurements over a range of concentrations of H₂SO₄ and VO²⁺. We provide empirical diffusion coefficients for these conditions in the hope of providing useful data for modelers that goes substantially beyond the few pieces of diffusion data in the literature and that helps to understand the variability in these data.

Though other researchers have reported cross-over of one or even multiple species through membranes,^{5,14,15} the analytical framework and experimental conditions were such that it is difficult to separate the multiple interactions occurring when several species are present. By proceeding through experiments utilizing one species at a time, as presented and analyzed within, we hope to extract more generally useful coefficients that can be translated from system to system. In addition, we report here a substantially wider range of compositions that have been used elsewhere, which we hope will be useful to modeling activities in the flow battery field. Such a range of data is often useful when integrating over composition gradients that develop during an experiment in the real system.

Experimental

An illustration of the experimental setup is shown in Figure 1. The cell used to monitor VO²⁺ permeability in this study was battery cell hardware purchased from Fuel Cell Technologies. A vanadium rich solution was flowed on one side of the membrane through a flow field while symmetrically on the other side a blank or vanadium deficit solution was flowed. The solutions were flowed using a Masterflex L/S

*Electrochemical Society Fellow.

^zE-mail: tzawodzi@utk.edu

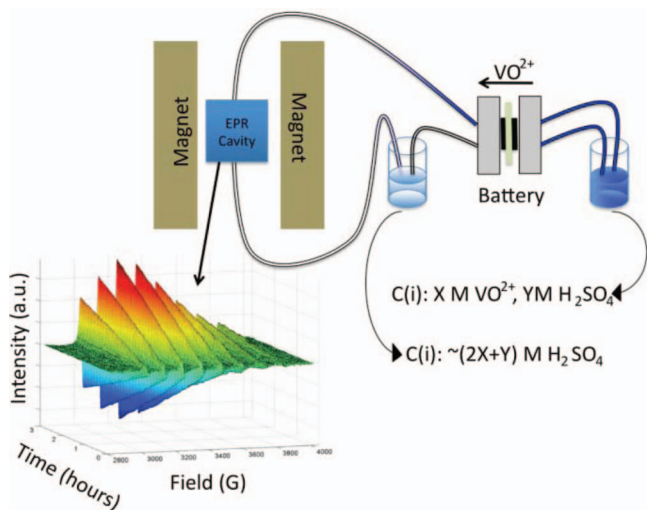


Figure 1. Illustration of experimental set up monitoring VO^{2+} crossover in the flow battery cell showing the resultant 3D plot of the increasing vanadium signal from the EPR with time.

four channel peristaltic pump system at 25 mL/min. The membrane used was a Nafion 117 membrane pretreated by heating to 75°C for 1 hour in 3% hydrogen peroxide followed by 1 hour in deionized water, 1 hour in 0.5 M sulfuric acid, and 1 hour in deionized water. The active area of the membrane was 5 cm². Teflon gaskets were used to create a 1 mil pooling area for the solutions inside the cell, as no electrodes were present.

Varying concentrations (0.1–0.8 M) of vanadyl sulfate (Alfa Aesar, 99.9%) were dissolved in varying concentrations (0.5–4 M) of sulfuric acid. The vanadium solutions were flowed through the cell with vanadium deficient solutions of sulfuric acid of a concentration matching the total cation concentration in the vanadium rich solution, taking into account the second dissociation constant of sulfuric acid. ‘Cation concentration’ was used to maintain a distinct terminology between the concentration of VO_2SO_4 and H_2SO_4 , as opposed to referring to sulfate concentration, which reflects on the concentrations of both species together. The ion balance was maintained to minimize osmotic pressure gradients. The volume of solution on both sides of the cell was 45 mL and was collected in volumetric cylinders so that any volume changes due to osmotic pressure driven water flow during the experiment could be monitored. Between crossover measurements the cell and tubing was thoroughly rinsed with DI water. The cell temperature was maintained at 30°C for all experiments.

The vanadium deficient side of the cell was flowed through the cavity of a Magnettech Miniscope EPR (Berlin, Germany). The VO^{2+} spectrum was monitored over time. Titration experiments shown in Figure 2, where the VO^{2+} concentration was increased over time and known at all times, confirm that the doubly integrated intensity of the VO^{2+} spectrum is linearly related to the concentration of VO^{2+} in solution. A spectrum of a standard of known VO^{2+} concentration was taken using the same parameters as the experiment to calculate the VO^{2+} concentrations from the EPR data. The EPR data was integrated and analyzed with scripts written in-house using the MathWorks’ MATLAB software.

The viscosity measurements were taken of solutions prepared from 0–2 M VO_2SO_4 and 0–5 M H_2SO_4 at 30–60°C. The viscometer used included a transparent thermostat CT 52 from SI analytics and an optical sensor.

Results

The doubly integrated intensity of the VO^{2+} spectra is linearly related to the concentration of VO^{2+} in the solution (Figure 2). Figure 3 shows an example of a crossover experiment monitored over long

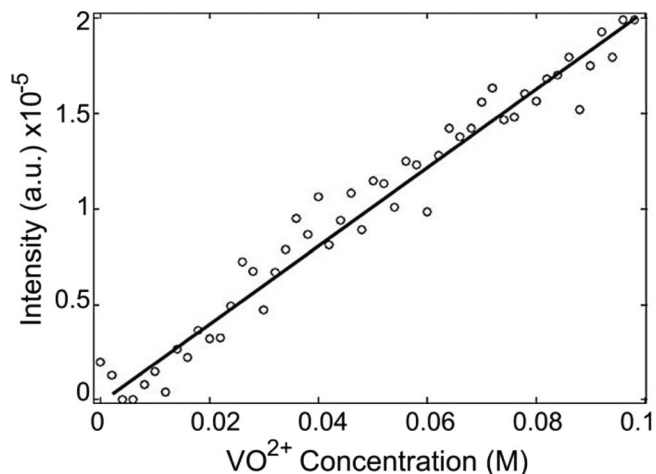


Figure 2. Linear relationship between doubly integrated intensity of VO^{2+} EPR signal and concentration from results of titration of VO^{2+} .

enough time for the VO^{2+} concentration on the vanadium deficient side of the cell to begin approaching equilibrium. This data was fit with a solution to Fick’s second law:¹⁶

$$C(t) = C_{t=\infty} + (C_{t=0} - C_{t=\infty})e^{-\frac{PA}{Vt}} \quad [1]$$

Where, given the experimental parameters set forth in this paper, $C_{t=0} = 0$ because the vanadium deficient (receiving) side of the battery is being monitored, $C_{t=\infty}$ is the equilibrium concentration, which is assumed to be $\frac{1}{2}$ the concentration of the vanadium rich side at time 0, A is the area of the membrane exposed to electrolyte, 5 cm² in this cell, V is the volume in mL of electrolyte on either side, l is the membrane thickness in m, t is time in s, and P is the permeability of the ion in the membrane in m²/s.

Shorter experimental times, on the order of 3 hours, provided adequate data for a reasonable fit to Equation 1. Figure 4 illustrates the results of monitoring the concentration change in the receiving compartment over the course of three hours. In this case the $[\text{VO}^{2+}]:[\text{H}_2\text{SO}_4]$ ratio was maintained at 1:5. Figure 4 shows the calculated concentration change from the EPR spectra and the fit with Eq. 1. Note that the highest VO^{2+} concentration accumulated on the vanadium deficient side at three hours was the result of the experiment with the lowest initial concentration in the vanadium rich side.

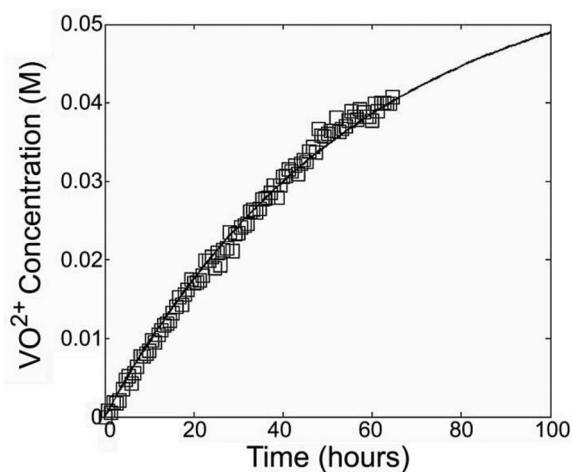


Figure 3. Concentration change in the vanadium deficient solution (0.7 M H_2SO_4) as VO^{2+} crossover occurs from the vanadium rich solution (0.1 M VO^{2+} , 0.5 M H_2SO_4) and the concentration approaches equilibrium. The line indicates the fit with Equation 1.

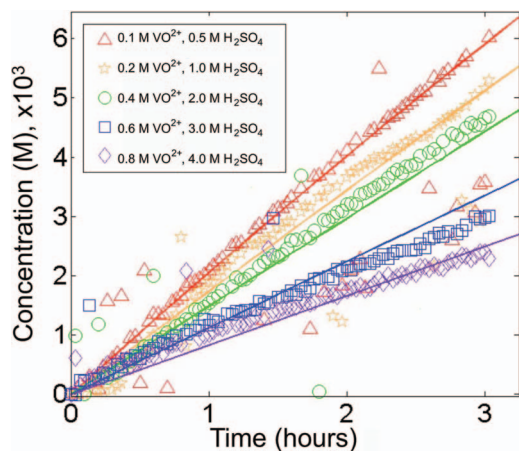


Figure 4. A. The concentration of VO^{2+} in the vanadium deficient side over three hours calculated from the doubly integrated EPR signal intensity for the $[\text{VO}^{2+}]:[\text{H}_2\text{SO}_4] = 1:5$ experiments. Lines show fit with Equation 1.

Figure 5 shows the change in VO^{2+} permeability with H_2SO_4 concentration with VO^{2+} concentration held constant and held at a constant 1:5 ratio with H_2SO_4 . Both decrease similarly with increased H_2SO_4 concentration. Figure 6 shows the effects of VO^{2+} concentration on VO^{2+} permeability with constant H_2SO_4 concentration. The VO^{2+} permeability of the constant H_2SO_4 /vanadium ratio is plotted as well for comparison. The diffusivity is related to the VO^{2+} permeability through the partitioning coefficient such that $P = KD$, where K is the partitioning coefficient.^{16,17} The partitioning coefficient is an important value not only to this experiment but also to battery operation, as it defines how much vanadium is allowed to enter the membrane in respect to the concentration of the outer solution, i.e. $P = C_{\text{membrane}}/C_{\text{solution}}$. A membrane with a very low vanadium partition coefficient would be ideal for battery operation.

The viscosity of a number of VO^{2+} and H_2SO_4 solutions was measured and the results are plotted in Figure 7 and listed in Table I. The Stokes-Einstein equation relates the diffusion constant of a species to the viscosity, η , of the solution:

$$D_{SE} = \frac{k_B T}{6\pi\eta r} \quad [2]$$

The curve in Figure 8 shows the prediction of Equation 2 with an 'effective' viscosity in the membrane defined at 3.29 times the solution viscosity. This factor was determined by scaling the data to match the

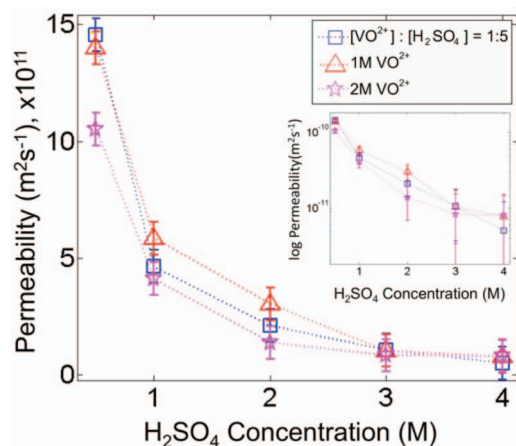


Figure 5. Permeability values calculated for changing H_2SO_4 concentrations for $[\text{VO}^{2+}]:[\text{H}_2\text{SO}_4] = 1:5$ (squares), 0.1 M VO^{2+} (triangles) and 0.2 M VO^{2+} (stars). The inset shows a log plot of the data.

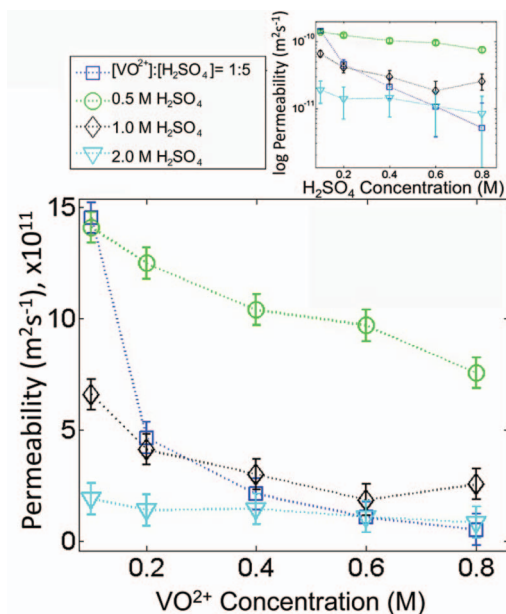


Figure 6. Permeability values calculated for changing VO^{2+} concentrations for $[\text{VO}^{2+}]:[\text{H}_2\text{SO}_4] = 1:5$ (squares), 0.5 M H_2SO_4 (circles), 1 M H_2SO_4 (diamonds) and 2 M H_2SO_4 (down pointing triangles). The inset shows a log plot of the data.

first, least concentrated and least viscous, point. This is meant as an illustration to show the extent of the departure of the experimental data to the theory.

In a separate calculation, the expected diffusivity was determined from Equation 2, using an effective viscosity in the membrane of 2.5 times that of the solution. The 2.5 value was determined by correcting the calculated VO^{2+} permeability of vanadium in water, with only minimal H_2SO_4 on the blank side of the cell to deter osmotic pressure, and matching the fraction of vanadium in the membrane to 50% of the total sulfonate groups in the membrane (as reported by Tang et al.¹⁸). Partition coefficients were determined from the VO^{2+} permeability data divided by the diffusivity values from Equation 2 ($K = P/D$). The density of the dry membrane (~ 1.8 g/L) was used to determine the number of sulfonate groups in the diffusion path to use the partitioning coefficients to determine a more tangible VO^{2+} partitioning fraction in the membrane. It is shown in Figure 9, along with VO^{2+} partitioning fraction values in Nafion calculated from data reported in Tang

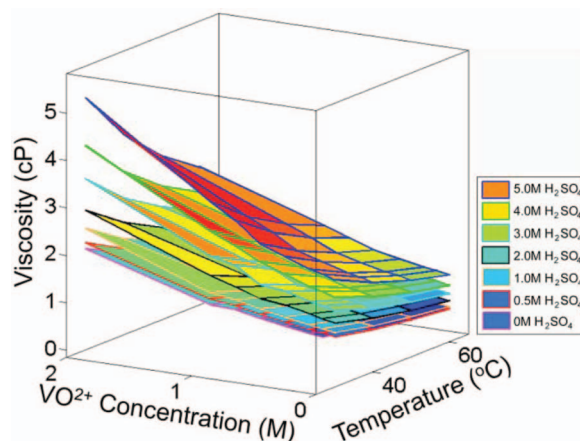


Figure 7. 3D plot of the viscosity data collected at 30–60°C for a range of VO^{2+} and H_2SO_4 concentrations. Data is in Table I.

Table I. Viscosity data collected at 30–60°C for a range of VO²⁺ and H₂SO₄ concentrations.

[VO ²⁺] (M)	[H ₂ SO ₄] (M)	Density (g/cm ³)	Visc. @ (cP)	30°C	40°C	50°C	60°C
0.1	0.0	1.017		0.855	0.701	0.589	0.505
0.2	0.0	1.022		0.888	0.730	0.616	0.530
0.4	0.0	1.047		0.972	0.797	0.670	0.575
0.6	0.0	1.062		1.057	0.862	0.726	0.618
0.8	0.0	1.088		1.166	0.950	0.792	0.674
1.0	0.0	1.083		1.196	0.970	0.809	0.687
2.0	0.0	1.190		1.988	1.578	1.290	1.068
0.0	0.1	1.015		0.834	0.687	0.580	0.498
0.0	0.5	1.032		0.894	0.735	0.619	0.537
0.1	0.5	1.053		0.941	0.772	0.651	0.558
0.2	0.5	1.057		0.973	0.801	0.676	0.582
0.4	0.5	1.077		1.055	0.866	0.728	0.627
0.6	0.5	1.095		1.147	0.938	0.786	0.672
0.8	0.5	1.114		1.254	1.020	0.852	0.727
1.0	0.5	1.124		1.312	1.064	0.888	0.754
2.0	0.5	1.207		2.106	1.670	1.363	1.141
0.0	1.0	1.069		0.987	0.813	0.683	0.588
0.1	1.0	1.082		1.029	0.845	0.711	0.610
0.2	1.0	1.091		1.076	0.885	0.746	0.642
0.4	1.0	1.106		1.159	0.951	0.801	0.689
0.6	1.0	1.123		1.256	1.026	0.861	0.738
0.8	1.0	1.139		1.374	1.117	0.932	0.800
1.0	1.0	1.150		1.439	1.165	0.977	0.826
2.0	1.0	1.232		2.411	1.880	1.526	1.270
0.0	2.0	1.134		1.185	0.976	0.822	0.707
0.1	2.0	1.149		1.245	1.026	0.867	0.748
0.2	2.0	1.165		1.309	1.077	0.907	0.785
0.4	2.0	1.169		1.415	1.158	0.972	0.832
0.6	2.0	1.169		1.475	1.202	1.005	0.856
0.8	2.0	1.201		1.640	1.333	1.112	0.945
1.0	2.0	1.212		1.806	1.460	1.212	1.027
2.0	2.0	1.283		2.789	2.211	1.790	1.490
0.0	3.0	1.196		1.447	1.183	0.995	0.857
0.1	3.0	1.215		1.517	1.248	1.052	0.906
0.2	3.0	1.209		1.567	1.287	1.083	0.930
0.4	3.0	1.222		1.710	1.398	1.172	1.005
0.6	3.0	1.216		1.769	1.437	1.197	1.017
0.8	3.0	1.256		2.098	1.698	1.407	1.195
1.0	3.0	1.269		2.217	1.791	1.483	1.254
2.0	3.0	1.352		3.463	2.729	2.228	1.846
0.0	4.0	1.245		1.731	1.427	1.200	1.031
0.1	4.0	1.264		1.820	1.498	1.263	1.084
0.2	4.0	1.253		1.879	1.542	1.295	1.113
0.4	4.0	1.275		2.071	1.694	1.418	1.213
0.6	4.0	1.287		2.250	1.831	1.528	1.297
0.8	4.0	1.319		2.512	2.027	1.680	1.421
1.0	4.0	1.330		2.744	2.214	1.832	1.548
2.0	4.0	1.387		4.159	3.288	2.665	2.213
0.0	5.0	1.304		2.100	1.727	1.453	1.249
0.1	5.0	1.312		2.186	1.799	1.518	1.303
0.2	5.0	1.308		2.251	1.854	1.556	1.335
0.4	5.0	1.314		2.441	2.001	1.669	1.425
0.6	5.0	1.345		2.633	2.155	1.804	1.543
0.8	5.0	1.360		3.043	2.461	2.039	1.726
1.0	5.0	1.382		3.368	2.716	2.245	1.892
2.0	5.0	1.442		5.169	4.075	3.306	2.738

et al., represented as a fraction of the sulfonate groups “occupied” by vanadium.

Discussion

The principle observations from this work are as follows:

1. VO²⁺ permeability decreases with increasing H₂SO₄ concentration.
2. VO²⁺ permeability decreases with increasing VO²⁺ concentration. However, as H₂SO₄ concentration increases, the effect of VO²⁺ concentration is diminished.
3. Viscosity of the solutions increases with concentration of all species and decreases with increasing temperature. The overall increase of viscosity with increasing concentration of one species (sulfuric acid or vanadium) is magnified at higher concentrations of the other species.

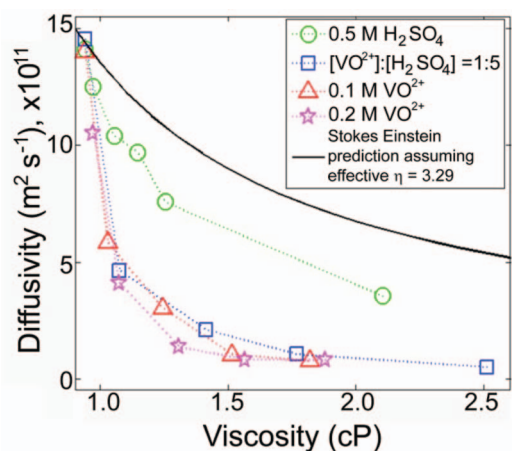


Figure 8. Plot of the viscosity measured for the electrolyte solutions vs. diffusivity (assuming partition coefficient of 1) data from the 0.5 M constant H_2SO_4 experiment, with $[\text{VO}^{2+}]$ increasing up to 2 M, the $[\text{VO}^{2+}]:[\text{H}_2\text{SO}_4] = 1:5$ experiment and the constant $[\text{VO}^{2+}]$ experiments. Line shows Stokes Einstein Debye prediction of diffusion assuming an effective viscosity in the membrane of 3.29 times the viscosity in the flowing solution.

- The increased viscosity of the bathing solutions caused either by increasing H_2SO_4 concentration or by increasing vanadium concentration is not alone responsible for the slower observed VO^{2+} permeability across the membrane with concentration.

As seen in Figures 5 and 6, the VO^{2+} permeability decreases with both increasing H_2SO_4 and VO^{2+} concentration. This effect becomes increasingly independent of VO^{2+} concentration as H_2SO_4 concentration increases. The viscosity of the electrolyte solutions increases with increasing H_2SO_4 concentration. In addition to viscosity changes, exposure to concentrated sulfuric acid solutions has a dehydrating effect on Nafion that intensifies with H_2SO_4 concentration.⁷ This occurs as the H_2SO_4 concentration increases beyond threshold of Donnan exclusion and some negatively charged species ('co-ions') can diffuse into the membrane.¹⁹ Donnan equilibrium theory suggests that for a membrane with evenly distributed fixed ion sites, ions in solution around the membrane of similar charge to that of the fixed site will be excluded if their concentration is less than that of charged sites in the membranes.²⁰ However, in Nafion and other ionomers used as polymer electrolytes, the ion sites are expected to form channels and/or

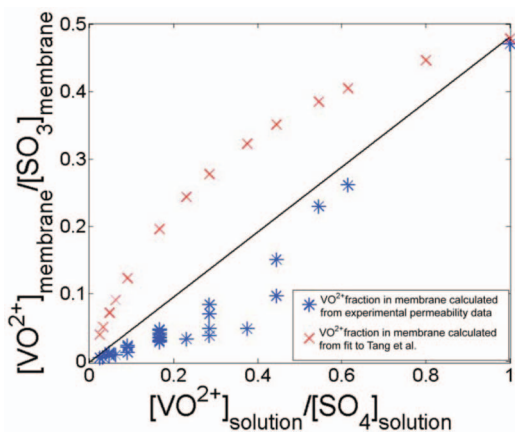


Figure 9. Fraction of VO^{2+} in the membrane per sulfonate group vs fraction of vanadium in the solution. The asterisks show the values calculated from the permeability data. Xs show values determined by fit to partitioning reported in Tang et al.¹⁸ The line represents the state where sulfonate occupation in the membrane reflects the amount of protons and VO^{2+} ions in solution.

clusters in the polymer matrix thereby increasing the local ion site concentration in the regions accessible to soluble ions. The effect of this structure is under investigation at present.

At lower H_2SO_4 concentrations, the concentration of vanadium in solution does show a small decrease in VO^{2+} permeability as VO^{2+} concentration increases. In Figure 6 it is evident that as H_2SO_4 concentration increases the effects of the VO^{2+} concentration become overshadowed by those due to the H_2SO_4 concentration itself. The effects of VO^{2+} concentration are nearly insignificant at 2 M sulfuric acid. The effects of VO^{2+} concentration at lower H_2SO_4 concentration may in part reflect an increase in viscosity in the electrolyte solution with increased ion concentration, leading to slower transport of the species to the membrane.

Previous studies have shown that VO^{2+} is incorporated into the membrane quickly upon exposure to VO^{2+} solution and increasing amounts of VO^{2+} in the membrane result in lower mobility of species in the membrane.²¹ In fact, VO^{2+} is still present in the membrane even after rinsing.⁹ Earlier studies of cation diffusion in Nafion have suggested two diffusion pathways for cations in the Nafion membrane: the swollen region and the ionic region. Cation diffusion is highly linked not just to water content but to free water content.^{22,23} Whether VO^{2+} diffuses through the membrane by site-to-site hopping or by free diffusion in solution of VO^{2+} that is unassociated with ion groups or a combination of these possibilities is still to be determined.

The values for VO^{2+} permeability in Figure 8 (or diffusivity if we consider, for the moment, equipartitioning of vanadium between the membrane and solution) in comparison to the trend predicted by the Stokes-Einstein relation show that even in the case of 0.5 M constant H_2SO_4 concentration (showing up to 2 M VO^{2+} to increase the viscosity to be comparable with higher H_2SO_4 concentrations) the measured values are systematically low and with increasing H_2SO_4 concentrations the difference is more pronounced. Possible reasons for this discrepancy include changes in partitioning with H_2SO_4 , higher effective viscosity in the membrane with more H_2SO_4 as a result of membrane dehydration and smaller effects of larger vanadium water clustering.

The acid interacting with the membrane does cause dehydration in the membrane. Mobility of species in the membrane substantially decreases as hydration decreases.²⁴⁻²⁶ The conductivity of the membrane also decreases with decreasing hydration.²⁷ However, the effects on species mobility of the moles of water in the membrane per mole of sulfonate, λ , can be described broadly in terms of two primary regimes of composition that differ with respect to the effect of hydration on diffusion in the membrane. For $\lambda < 8$, stronger ion-ion interaction effects and closer vicinity of polar and charged particles result in a large change of diffusion rates with changing λ . When $\lambda > 8$, a substantially weaker dependence of mobility on λ is observed.²⁸ Previous reports show that λ decreases to ~ 10 with exposure to the highest H_2SO_4 concentrations used in this study.¹⁹ While the decrease in water content would certainly affect the diffusivity of VO^{2+} in the membrane, the hydration level is still in a realm where the hydration has a lesser effect on diffusion.

While the presence of VO^{2+} in the membrane has been observed to have little to no effect on the hydration level, the effect of VO^{2+} present in the membrane on diffusivity of chemical species and conductivity of the membrane is consistent with previous observations.^{9,18,19} Nonetheless, how this affects the diffusivity pattern (i.e. do diffusivity changes in the presence of VO^{2+} become more extreme at higher λ due to some water molecules hydrating the VO^{2+} instead of the membrane) needs to be more fully understood.

The permeability of a diffusing species is considerably affected by the partitioning coefficient.¹⁷ In Figure 9 we show the results of calculating an effective partition coefficient by assuming that the deviation from a Stokes-Einstein model is caused by changes in the partition coefficient. This data is compared with predicted vanadium fraction in the membrane values calculated from a fit to partitioning data of Tang et al.¹⁸ While the work of Tang et al., which measured the vanadium uptake directly, shows a preference for VO^{2+} to diffuse into the membrane over protons, here the predicted partitioning is shown as slightly

less preferential than the proton. A rationalization of this discrepancy is that a fraction of the VO^{2+} in the membrane is in fact immobilized by interacting strongly with sulfonate sites and thus diffuses exceedingly slowly. This would make the apparent partitioning based on a mobility comparison lower than what is observed when all vanadium (mobile and immobile) is stripped from the membrane, such as in Tang et al. Anderson and coworkers¹⁷ reported similar observations of mobile and immobile species in polyacrylamide gels.

Ultimately, to improve battery operation and efficiency, a membrane with high proton conductivity and low VO^{2+} permeability as well as good stability is essential. In the case of the VRFBs, e.g. in comparison to the highly studied methanol crossover problem of direct methanol fuel cells, the membrane is exposed to a larger number of different components. In the VRFB system, what we observe with increased exposure to vanadium and sulfuric acid can be caused by a) dehydration of the membrane, b) bisulfate and sulfate groups diffusing into the membrane c) vanadium exchanging with protons at the fixed ion groups in the membrane or d) increases in the local viscosity in the membrane. From the data presented in this study, it is difficult to sort amongst these possibilities to identify a root cause for our observations.

Determining what combination of these effects inhibits crossover can ultimately guide membrane development for the specific application of VRFBs. Further understanding of viscosity and species partitioning/clustering in the electrolyte solutions as well as battery performance as a result of changing H_2SO_4 concentration are needed to continue to improve operation conditions. The crossover of ion species from one side to the other side of the membrane is linked with the crossover of another species in the opposite direction. Characterization of the permeability of all vanadium species in the battery in the absence and presence of the other species is necessary.

Conclusions

Vanadium ion permeation through Nafion was studied as a function of the composition of the bathing solution. The results indicate rather slow permeation rates of vanadium ions through this membrane. The H_2SO_4 concentration of the solution has a significant effect on ion permeability in Nafion membranes. The effects of H_2SO_4 concentrations are so strong as to overshadow the effects of VO^{2+} concentration and temperature as H_2SO_4 concentration approaches 2 M. While the acid effects that decrease permeability of the VO^{2+} are also expected

to negatively affect the conductivity, there may be a beneficial concentration that balances these effects. Detailed, molecular level interpretation of these observations awaits further studies of partitioning and local mobility within the membrane.

References

1. M. Rychcik and M. Skyllas-Kazacos, *Journal of Power Sources*, **22**, 59 (1988).
2. D. S. Aaron, Z. Tang, A. B. Papandrew, and T. A. Zawodzinski, *J. Appl. Electrochem.*, **41**, 1175 (2011).
3. V. Haddadi-Asl, M. Kazacos, and M. Skyllas-Kazacos, *J. Appl. Electrochem.*, **25**, 29 (1995).
4. J. Xi, Z. Wu, X. Teng, Y. Zhao, L. Chen, and X. Qiu, *Journal of Materials Chemistry*, **18**, 1232 (2008).
5. C. Sun, J. Chen, H. Zhang, X. Han, and Q. Luo, *Journal of Power Sources*, **195**, 890 (2010).
6. S. Kim, J. Yan, B. Schwenzer, J. Zhang, L. Li, J. Lui, Z. Yang, and M. Hickner, *Electrochemistry Communications*, **12**, 1650 (2010).
7. M. W. Verbrugge and R. F. Hill, *J. Phys. Chem.*, **92**, 6778 (1988).
8. M. W. Verbrugge and R. F. Hill, *J. Electrochem. Soc.*, **137**, 886 (1990).
9. J. Lawton, D. S. Aaron, Z. Tang, and T. A. Zawodzinski, *J. Mem. Sci.*, **428**, 38 (2013).
10. A. A. Shah, H. Al-Fetlawi, and F. C. Walsh, *Electrochimica Acta*, **55**, 1125 (2010).
11. D. You, H. Zhang, and J. Chen, *Electrochimica Acta*, **54**, 6827 (2009).
12. A. A. Shah, M. J. Watt-Smith, and F. C. Walsh, *Electrochimica Acta*, **53**, 8087 (2008).
13. A. Tang, J. Bao, and M. Skyllas-Kazacos, *J. Power Sources*, **196**, 10737 (2011).
14. B. Schwenzer, S. Kim, M. Vijaykumar, Z. Yang, and J. Liu, *J. Mem. Sci.*, **372**, 11 (2011).
15. K. W. Knehr, A. Ertan, C. R. Dennison, A. R. Kalidindi, and E. C. Kumbar, *J. Electrochem. Soc.*, **159**, A1446 (2012).
16. J. Crank, *The Mathematics of Diffusion*, Oxford University Press, New York (1975).
17. J. Tong and J. L. Anderson, *Biophys. J.*, **70**, 1505 (1996).
18. Z. Tang and T. A. Zawodzinski (2012).
19. Z. Tang, R. Keith, D. S. Aaron, J. Lawton, A. B. Papandrew, and T. A. Zawodzinski, *ECS Transactions*, **41**, 25 (2012).
20. W. Y. Hsu and T. D. Gierke, *J. Mem. Sci.*, **13**, 307 (1983).
21. R. C. Barklie, O. Girard, and O. Braddell, *Journal of Physical Chemistry*, **92**, 1371 (1988).
22. G. Pourcelly, P. Sistat, A. Chapotot, C. Gavach, and V. Nikonenko, *J. Mem. Sci.*, **110**, 69 (1996).
23. M. A. Spitsyn, V. N. Andreev, V. E. Kazarinov, D. V. Kokoulina, and L. I. Krishalikh, *Elektrokhimiya*, **20**, 1063 (1984).
24. S. J. Paddison, P. Reginald, and T. A. Zawodzinski, *J. Chem. Phys.*, **115**, 7753 (2001).
25. J. S. Lawton and D. E. Budil, *Journal of Physical Chemistry B*, **113**, 10679 (2009).
26. T. A. Zawodzinski, M. Neeman, L. O. Sillerud, and S. Gottesfeld, *J. Phys. Chem.*, **95**, 6040 (1991).
27. G. Alberti, U. Costantino, M. Casciola, R. Ferroni, L. Massinelli, and P. Staiti, *Solid State Ionics*, **145**, 249 (2001).
28. T. A. Zawodzinski, C. Derouin, S. Radzinski, R. J. Sherman, V. T. Smith, T. E. Springer, and S. Gottesfeld, *J. Electrochem. Soc.*, **140**, 1041 (1993).